Cell, Vol. 106, 157–169, July 27, 2001, Copyright ©2001 by Cell Press

Plasma Membrane Repair Is Mediated by Ca^{2+}-Regulated Exocytosis of Lysosomes

Anita Reddy, Elisabet V. Caler, and Norma W. Andrews[1]
Section of Microbial Pathogenesis
Boyer Center for Molecular Medicine
Yale University School of Medicine
New Haven, Connecticut 06520

Summary

Plasma membrane wounds are repaired by a mechanism involving Ca^{2+}-regulated exocytosis. Elevation in intracellular [Ca^{2+}] triggers fusion of lysosomes with the plasma membrane, a process regulated by the lysosomal synaptotagmin isoform Syt VII. Here, we show that Ca^{2+}-regulated exocytosis of lysosomes is required for the repair of plasma membrane disruptions. Lysosomal exocytosis and membrane resealing are inhibited by the recombinant Syt VII C_2A domain or anti-Syt VII C_2A antibodies, or by antibodies against the cytosolic domain of Lamp-1, which specifically aggregate lysosomes. We further demonstrate that lysosomal exocytosis mediates the resealing of primary skin fibroblasts wounded during the contraction of collagen matrices. These findings reveal a fundamental, novel role for lysosomes: as Ca^{2+}-regulated exocytic compartments responsible for plasma membrane repair.

Introduction

Restoration of plasma membrane integrity after injury is essential for the survival of animal cells. It is well documented that plasma membrane damage followed by rapid repair occurs frequently, in a variety of settings. Fibroblasts locomoting in culture, for example, often rupture their plasma membrane during retraction of the trailing edge, but the lesion is repaired in a few seconds (Chen, 1981). Fibroblasts contracting collagen matrices, a process essential for wound healing in vivo, also form transient plasma membrane disruptions, which rapidly reseal (Lin et al., 1997). In rodents, cells from tissues routinely subjected to mechanical stress (such as skin, gut, and muscle) are also injured, as demonstrated by the incorporation of membrane-impermeant molecules into their cytosol (McNeil and Ito, 1989; McNeil and Khakee, 1992; McNeil and Steinhardt, 1997). In skeletal muscle, in particular, the frequency of wounding was found to be a function of the mechanical load applied to the cells (McNeil and Khakee, 1992). Another dramatic example of resealing capacity is provided by injured sea urchin eggs. Large sections of plasma membrane can be removed, and, within a few seconds, these eggs are again completely impermeable to extracellular Ca^{2+} and can be fertilized and divide (Terasaki et al., 1997). Furthermore, it is widely known that laboratory techniques such as scrape-loading, microinjection, and electroporation efficiently deliver macromolecules into the cytosol of cells through reversible plasma membrane disruptions (McNeil et al., 1984; McNeil and Warder, 1987; Miyake and McNeil, 1995).

Plasma membrane repair was originally thought to be mediated by the thermodynamically-favored partitioning of hydrophobic phospholipid groups away from the aqueous environment. This notion was supported by the spontaneous resealing observed in erythrocyte ghosts and liposome vesicles (Chang and Reese, 1990). However, complete resealing in erythrocyte ghosts is a very slow process (Lee et al., 1985; Lieber and Steck, 1982) that does not require Ca^{2+}, and is facilitated by Mg^{2+} (Bodemann and Passow, 1972). Mammalian cells, in contrast, reseal plasma membrane disruptions within 10–30 s, and the process is strictly dependent on extracellular Ca^{2+}, and antagonized by Mg^{2+} (McNeil and Steinhardt, 1997; Steinhardt et al., 1994). Such important differences established that plasma membrane repair in nucleated cells is a more complex and tightly regulated process, initiated by Ca^{2+} influx from the extracellular medium.

A series of studies in the last decade suggested that plasma membrane repair in animal cells is mediated by the delivery of intracellular membrane to wound sites, by a mechanism resembling Ca^{2+}-regulated exocytosis. Observations in endothelial cells, fibroblasts, and sea urchin eggs showed that Ca^{2+} influx through plasma membrane disruptions triggers a high rate of vesicular exocytosis at the wound site, an event required for membrane resealing (Bi et al., 1995; Miyake and McNeil, 1995; Steinhardt et al., 1994). Intracellular membrane delivery has been shown to reduce plasma membrane tension (Dai and Sheetz, 1995), suggesting a mechanism by which exocytosis could promote resealing (Togo et al., 1999, 2000). These studies therefore pointed to a ubiquitous form of Ca^{2+}-regulated exocytosis as a necessary and rate-limiting step in plasma membrane repair (Bi et al., 1995; Miyake and McNeil, 1995).

Although Ca^{2+}-regulated exocytosis was generally considered to be present only in specialized secretory cells, recent studies revealed the presence of a large, Ca^{2+}-triggered exocytic component in a variety of cells, including fibroblasts and epithelial cells (Chavez et al., 1996; Coorsen et al., 1996; Ninomiya et al., 1996). Even in cells known to contain specialized secretory granules, such as PC-12 cells, an additional population of Ca^{2+}-regulated exocytic vesicles was detected, with properties distinct from the classical dense-core or synaptic-like granules (Kasai et al., 1999). Such studies reinforced the growing perception that most cell types contain a population of vesicles that can be mobilized for fusion with the plasma membrane upon elevation in $[Ca^{2+}]_i$.

Recent studies in NRK and other cell types showed that these ubiquitous Ca^{2+}-regulated secretory vesicles correspond to conventional lysosomes (Andrews, 2000; Rodríguez et al., 1997, 1999). It thus became a question of great biological interest to elucidate the physiological role of this ubiquitous, Ca^{2+}-regulated lysosomal exocytic pathway. Here, we present evidence indicating that

[1] Correspondence: norma.andrews@yale.edu

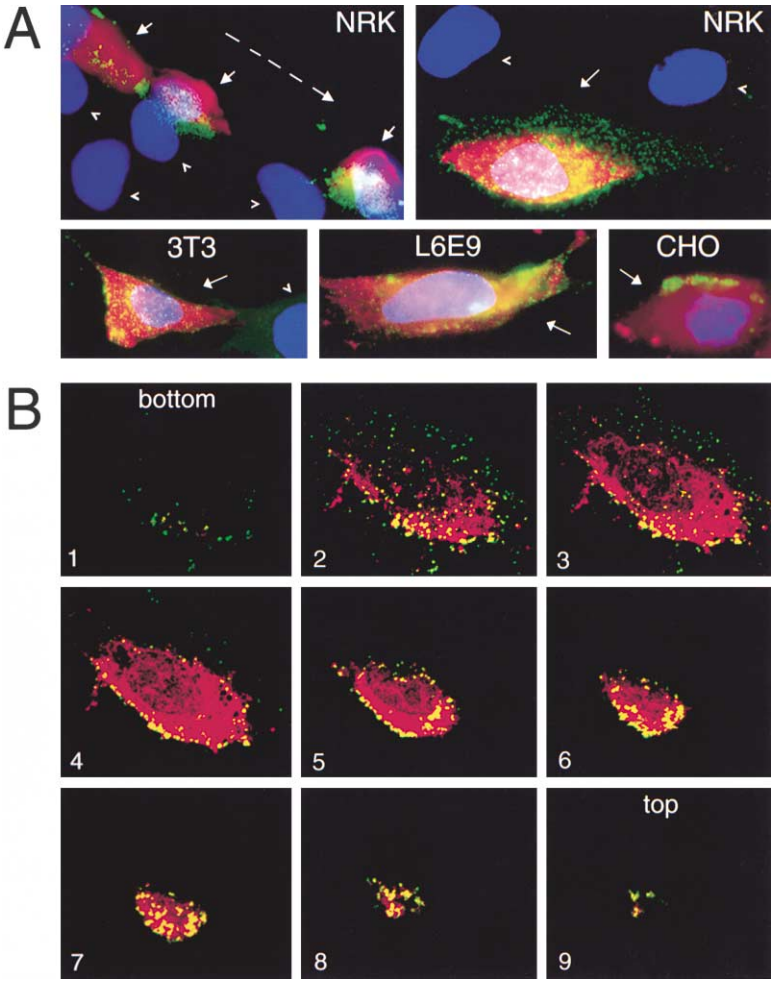

Figure 1. The Lumenal Domain of Lamp-1 Is Exposed on the Surface of Wounded Cells

(A) NRK, 3T3, L6E9, and CHO cells were wounded by scratching in the presence of Texas-Red dextran, and labeled at 4°C with anti-Lamp-1 lumenal domain mAbs. Red corresponds to the dextran incorporated into the cytosol of wounded cells, green to the punctate anti-Lamp-1 surface label, and blue to DAPI staining of nuclei. Arrows point to wounded cells positive for surface Lamp-1; arrowheads point to nonwounded cells in the same microscopic field. The interrupted line arrow indicates where scratching occurred.

(B) Confocal Z-series of a wounded NRK cell (cytosolic dextran in red) with Lamp-1 staining on the plasma membrane (anti-Lamp-1 mAb in green). Optical sections 1–9 were taken in series from the bottom to the top of the cell.

Ca^{2+}-dependent lysosomal exocytosis plays an essential role in the mechanism by which mammalian cells reseal their plasma membrane after injury.

Results

Wounding Induces Surface Exposure of the Major Lysosomal Membrane Glycoprotein Lamp-1 at the Wound Site

To investigate the involvement of lysosomal exocytosis in plasma membrane repair, exposure of the lumenal domain of Lamp-1 on the surface of NRK cells was examined after wounding. Lamp-1 is an abundant lysosomal membrane glycoprotein, normally not present on the plasma membrane of NRK cells (Harter and Mellman, 1992). When lysosomes are induced to fuse with the plasma membrane by elevation in the intracellular free Ca^{2+} concentration $[Ca^{2+}]_i$, the intralysosomal NH_2-terminal domain of Lamp-1 becomes exposed on the cell surface. This fusion event can be specifically detected by surface-staining live cells with monoclonal antibodies (mAbs) directed to a lumenal epitope of Lamp-1 (Martinez et al., 2000; Rodríguez et al., 1997).

NRK cells were wounded by scratching with a surgical blade in Ca^{2+}-containing PBS, in the presence of lysine-fixable Texas Red-dextran. This previously described procedure generates wounded cells that are easily identified by intracellular incorporation of the dextran tracer (Swanson and McNeil, 1987). Cell wounding was immediately followed by transfer to ice and surface staining for the lumenal domain of Lamp-1. As expected, wounded cells (identified based on Texas Red-dextran cytoplasmic staining) were concentrated along the edges of scratch marks. Punctate surface Lamp-1 staining was detected on NRK cells wounded by scratching, but not on nonwounded cells in the same microscopic field (Figure 1A, top). Similar results were obtained in scratch assays using three additional cell lines: 3T3 mouse fibroblasts, L6E9 rat myoblasts and CHO hamster ovary cells (Figure 1A, bottom). Confocal optical Z-sectioning confirmed that the punctate Lamp-1 immunostaining was localized on the plasma membrane of wounded NRK cells (Figure 1B).

In several of the scratch-wounded cells, the Lamp-1 surface staining appeared to be concentrated on plasma membrane regions close to the wound site. To confirm this observation, NRK cells were wounded by microinjecting a Texas Red-dextran solution. After microinjection, the cells were immediately transferred to ice and surface-stained for the Lamp-1 lumenal domain. After fixation, a "track" mark formed by the injected Texas Red-dextran solution was apparent in the cells, allowing

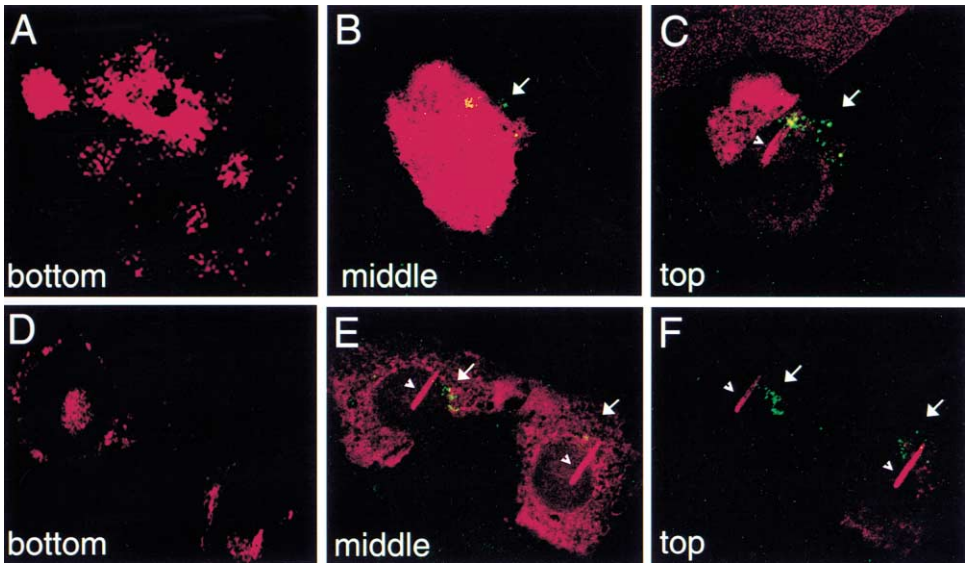

Figure 2. The Lumenal Domain of Lamp-1 Is Exposed on the Cell Surface at the Wound Site

Images from two independent confocal Z series are shown (A–C) and (D–F), corresponding to bottom, middle, and top optical sections of NRK cells microinjected with Texas Red-dextran (red cytosolic labeling) and surface stained for the lumenal domain of Lamp-1. Arrowheads in (C), (E), and (F) point to dextran-stained microinjection "tracks". Arrows point to localized areas stained with the anti-Lamp-1 mAb (green), next to needle puncture sites.

precise localization of the microneedle puncture site (Figures 2C, 2E, and 2F). In the majority of microinjected cells, the entry site of the needle "track" corresponded closely to regions positively stained for the lumenal epitope of Lamp-1. Confocal Z-sectioning showed that Lamp-1 immunostaining was primarily detected on the uppermost optical sections, where wounding occurred (Figures 2C and 2F, green punctate staining), and absent from bottom sections of the cells (Figures 2A and 2D). In several independent experiments, surface-exposed Lamp-1 was detected close to the sites of plasma membrane puncture, on 60%–70% of the microinjected cells. The remaining microinjected cells, as well as all noninjected cells, had no detectable Lamp-1 staining (not shown).

Lamp-1 Exposure on the Cell Surface after Wounding Requires Extracellular Ca^{2+}

Both lysosomal exocytosis and plasma membrane repair have been reported to be Ca^{2+}-dependent events (Bi et al., 1995; Miyake and McNeil, 1995; Rodríguez et al., 1997). We thus investigated whether extracellular Ca^{2+} was required for exposure of the lumenal domain of Lamp-1 on the plasma membrane after wounding. After scratch-wounding in the presence of Ca^{2+} and surface immunostaining, 83% of wounded NRK cells present along the scratch marks had detectable Lamp-1 on the surface (Figures 3A and 3B). However, when cells were wounded in the presence of 10 mM EGTA, only 22% of wounded cells were positive for surface Lamp-1 (Figures 3A and 3B).

In the experiments described above, we observed a significant reduction (of almost 50%) in the number of cells remaining attached to the coverslip after wounding in the presence of EGTA (N, Figure 3B), suggesting that the degree of inhibition in Lamp-1 surface exposure was probably underestimated. To quantitatively and more accurately analyze the total detectable amount of surface Lamp-1 on larger cell populations immediately after wounding, NRK cells were wounded and removed from the dish simultaneously by scraping in the presence of fluorescent dextran. This wounding technique, also known as "scrape loading," results in efficient introduction of membrane-impermeant molecules into the cytosol of cells, and has been widely used for this purpose (McNeil et al., 1984). Cells scraped in the presence or absence of extracellular Ca^{2+} were surface labeled in suspension for the lumenal epitope of Lamp-1, fixed and analyzed by flow cytometry (FACS). As shown in Figure 3C, 96%–97% of the cell population scraped in the presence of Ca^{2+} was wounded, as judged by uptake of BODIPY FL-dextran. Of these wounded cells, 49% had detectable surface staining with anti-Lamp-1 lumenal domain mAbs (Figure 3C, Ca^{2+}). In contrast, in the absence of extracellular Ca^{2+}, 99% of the cells were initially wounded, but only 5% of these had detectable Lamp-1 on the cell surface (Figure 3C, EGTA).

The Lumenal Domain of the Lysosomal Synaptotagmin Isoform Syt VII Is Exposed on the Cell Surface after Wounding

Members of the synaptotagmin family of Ca^{2+} binding proteins have been proposed to play a central role in the regulation of Ca^{2+}-dependent exocytosis in neurons and other cell types (Schiavo et al., 1998; Sudhof and Rizo, 1996). Synaptotagmins have a short N terminus lumenal domain (ectodomain), a transmembrane region, and two Ca^{2+} binding cytosolic domains, C_2A and C_2B, homologous to the C_2 domain of protein kinase C (Sudhof and Rizo, 1996). The synaptotagmin C_2A domains,

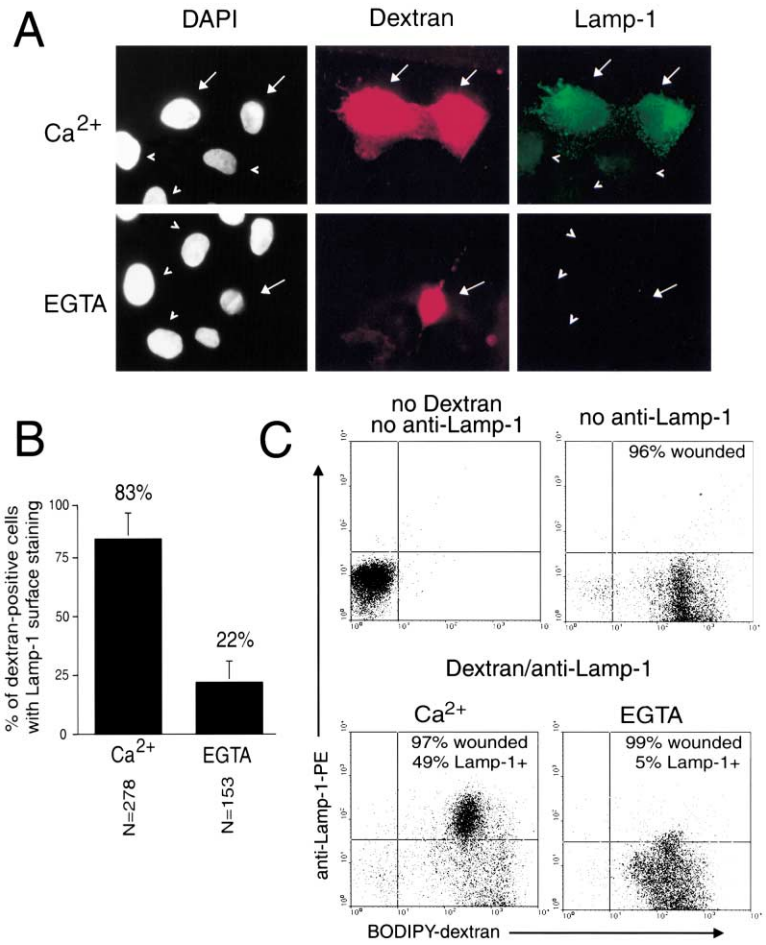

Figure 3. Exposure of Lamp-1 on the Surface of Wounded Cells Requires Extracellular Ca^{2+}

(A) NRK cells were wounded by scratching in the presence of Texas-Red dextran in buffer containing Ca^{2+} or EGTA, and labeled at 4°C with anti-Lamp-1 lumenal domain mAbs (green). Arrows point to wounded cells (red), and arrowheads to nonwounded cells in the same field (DAPI).

(B) The number of wounded NRK cells with surface-exposed Lamp-1 was quantified visually, and plotted as a percentage of the total number of wounded cells. N = total number of wounded cells counted.

(C) FACS analysis of NRK cells wounded by scraping in the presence of BODIPY-dextran and labeled at 4°C with anti-Lamp-1 mAbs, followed by R-Phycoerythrin (PE)-secondary antibody. No anti-Lamp-1 and no dextran/no anti-Lamp-1 controls are shown (top panels).

in particular, have been strongly implicated in the regulation of exocytosis (Mikoshiba et al., 1995, Sugita and Sudhof, 2000). The ubiquitously expressed synaptotagmin isoform Syt VII (Li et al., 1995; Ullrich and Sudhof, 1995) is localized on the membrane of lysosomes in several cell types (Caler et al., 2001; Martinez et al., 2000). Recombinant peptides containing the Syt VII C_2A domain or antibodies against this domain inhibit Ca^{2+}-triggered lysosomal exocytosis in permeabilized cells (Martinez et al., 2000). In NRK cells, Syt VII was detected on dense vesicles containing the lysosomal glycoprotein Lamp-1 but not the late endosomal marker rab-7, suggesting that Syt VII is present on mature lysosomes and not on late endosomes (Caler et al., 2001; Martinez et al., 2000).

To investigate a potential role for Syt VII in wounding-associated lysosomal exocytosis, we initially verified if the lumenal domain of Syt VII was exposed on the plasma membrane after wounding. NRK cells were scratch wounded in the presence of Texas Red-dextran, and surface stained at 4°C with rabbit antibodies against the NH_2-terminus of Syt VII (isoform specific ectodomain). Whereas no staining was detected on nonwounded cells, wounded NRK cells were specifically labeled with the anti-Syt VII ectodomain antibodies, indicating that this lumenal domain was exposed on the cell surface. No surface staining was detected when cells were labeled with preimmune rabbit antibodies (Figure 4A, top panels). To confirm the specificity of the surface staining assay, live NRK cells wounded by scratching in the presence of Texas Red-dextran were incubated at 4°C with antibodies specific for the cytosolic C_2A domain of Syt VII. As expected, these antibodies did not stain wounded cells, confirming that the cytosolic C_2A domain of Syt VII is not exposed on the cell surface after lysosomal exocytosis. However, when wounded cells were fixed and permeabilized, staining was detected with anti-Syt VII C_2A antibodies on intracellular lysosomes (Figure 4A, lower panels), as previously reported (Martinez et al., 2000). The ectodomain of Syt VII was also specifically detected on the surface of wounded CHO and L6E9 cells (not shown).

Wounding-Induced Exocytosis of Lysosomes and Plasma Membrane Resealing Are Regulated by the Syt VII C_2A Domain

The results above showed that Syt VII is present on the membrane of the same Lamp-1-positive lysosomal population which fuses with the plasma membrane after wounding. We next examined if wounding-mediated lysosomal exocytosis was affected by modulation of Syt VII function. Scrape-wounding assays were performed with NRK cells in the presence of recombinant C_2A domains of Syt VII or, as a control, the exclusively neuronal isoform Syt I, followed by Lamp-1 surface staining and FACS analysis. As shown in Figure 4B (middle), there was a marked reduction in surface-exposed Lamp-1 in cells wounded in the presence of Syt VII C_2A, but not in

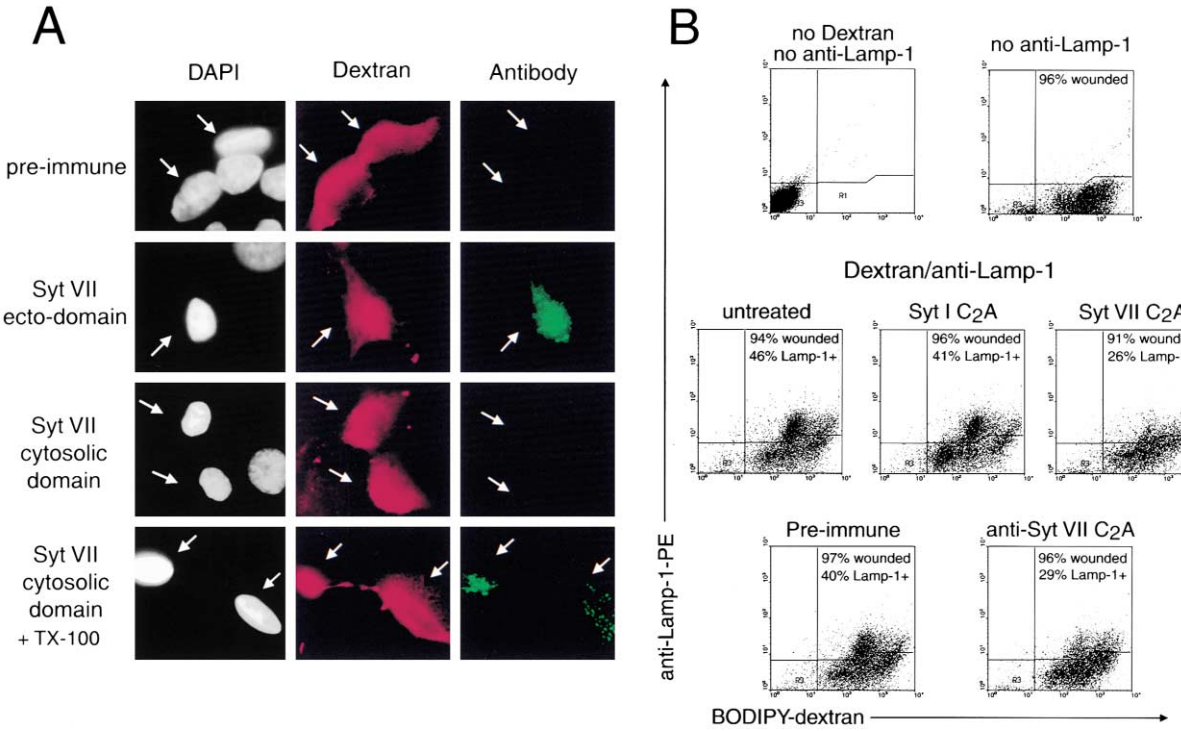

Figure 4. Syt VII Regulates Surface Exposure of Lamp-1 in Wounded Cells

(A) NRK cells were wounded by scratching in the presence of Texas-Red dextran and labeled at 4°C with preimmune, anti-Syt VII ectodomain, or anti-Syt VII C_2A cytosolic domain antibodies. Surface labeling was only detected with anti-Syt VII ectodomain antibodies (green, second row). After fixation and permeabilization, staining was detected with anti-Syt VII C_2A cytosolic domain antibodies (green, bottom row). Arrows point to wounded cells (red).

(B) NRK cells were wounded by scraping and analyzed by FACS. Top row, no dextran and no dextran/no anti-Lamp-1 controls; middle and lower rows, cells scraped in the presence of BODIPY-dextran and surface labeled with anti-Lamp-PE, in the absence or presence of Syt I C_2A, Syt VII C_2A, preimmune, or anti-Syt VII C_2A IgG.

cells scraped in the presence of the same concentration of Syt I C_2A. Similarly, inhibition of the total amount of Lamp-1 detectable on the cell surface was observed when cells were scrape wounded in the presence of affinity-purified anti-Syt VII C_2A antibodies, but not in the presence of preimmune rabbit antibodies (Figure 4B, bottom).

We proceeded to examine the role of Syt VII-dependent lysosomal exocytosis in plasma membrane resealing, using an assay based on sequential uptake of two different fluorescent-labeled dextrans. In these experiments, plasma membrane disruptions were induced by contact with glass beads, a technique that allows microscopic examination of large numbers of wounded cells attached to coverslips (McNeil and Warder, 1987). Glass beads were sprinkled on NRK cell monolayers in the presence of Texas Red-dextran (first tracer) and coverslips were either washed and immediately incubated with BODIPY FL-dextran (second tracer) for 15 s, or transferred to 37°C for 1 and 3 min, and then incubated with BODIPY FL-dextran for 15 s before fixation. Cells that were injured by contact with the glass beads took in the first tracer (Figure 5A, top panels—the areas marked by asterisks correspond to the sites where beads disrupted the monolayer). Consistent with previous observations (Eddleman et al., 1997), a fraction of the wounded cell population was also stained with the second tracer immediately after wounding, indicating that open membrane lesions were still present. However, after further incubation at 37°C for 1 min, the majority of the wounded cells stained by the first tracer had resealed most of their membrane disruptions, as reflected by the exclusion of the second tracer (Figure 5A, lower panels). When cells were wounded and subsequently incubated in the presence of recombinant Syt I C_2A, the results were very similar: the fraction of wounded cells that took up the second tracer was significantly reduced after 1 min incubation at 37°C. In contrast, wounding and incubation in the presence of Syt VII C_2A produced dramatically different results: The majority of wounded cells stained by the first tracer were also stained by the second tracer immediately after wounding (Figure 5A, top panels), and this proportion did not change significantly after 1 min at 37°C (Figure 5A, lower panels). Thus, a larger proportion of the cells injured in the presence of the inhibitory Syt VII C_2A fragments appeared unable to exclude the second tracer, suggesting that Syt VII function is required for efficient membrane resealing.

The observations above were confirmed by counting the number of wounded cells labeled by the second tracer after 0, 1, and 3 min at 37°C. About 60% of the cells wounded in the presence or absence of Syt I C_2A were resistant to loading with the second tracer immediately, and this proportion rose to 80%–90% with increased periods of incubation at 37°C (Figure 5B). In

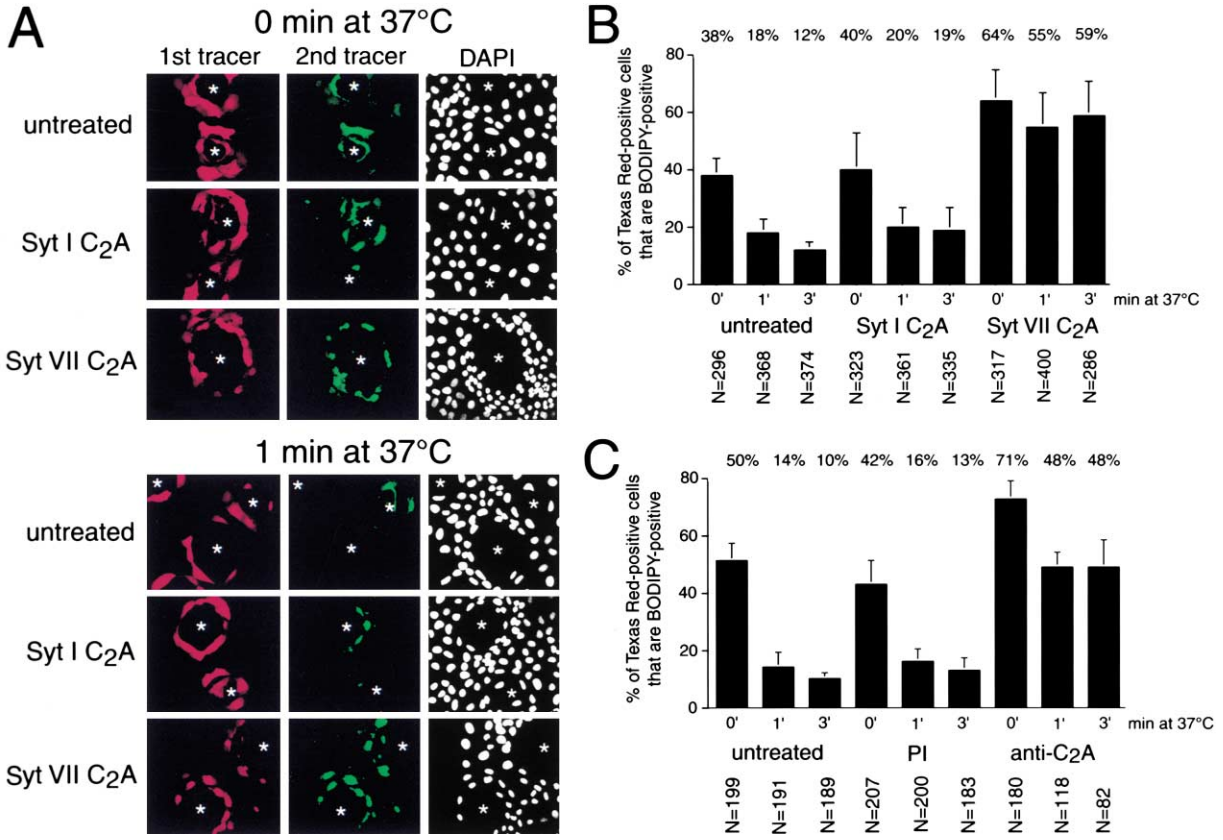

Figure 5. Recombinant Syt VII C_2A and anti-Syt VII C_2A Antibodies Inhibit Plasma Membrane Resealing

(A) NRK cells were wounded by contact with glass beads in the presence of Texas Red-dextran (red, first tracer), and exposed to BODIPY-dextran (green, second tracer) immediately (0 min) or after 1 min at 37°C. DAPI stain indicates nuclei of all cells in field.

(B and C) The number of glass bead-wounded NRK cells (Texas Red-dextran-positive) labeled with the second tracer (BODIPY-dextran-positive) was quantified visually, and plotted as a percentage of the total number of wounded cells. N = total number of Texas Red-dextran-containing wounded cells counted in 3 (B) or 2 (C) separate experiments. The presence of Syt I C_2A, Syt VII C_2A, preimmune or anti-Syt VII C_2A antibodies during wounding and additional incubation at 37°C are indicated.

contrast, only 36% of the cells wounded in the presence of Syt VII C_2A excluded the second tracer immediately, and this fraction did not increase significantly with further incubation at 37°C (Figure 5B). Very similar results were obtained when the cells were wounded in the presence of anti-Syt VII C_2A domain antibodies (Figure 5C). Importantly, however, a significant fraction of the cells wounded and maintained in the presence of the anti-C_2A antibodies detached from the coverslip during incubation at 37°C (N, Figure 5C). This loss was specific for wounded cells, since there was no change in the total number of dextran-negative, nonwounded cells, as determined by DAPI staining (not shown). These observations strongly suggest that the size of the nonsealed cell population was underestimated in these experiments, and that the viability of cells wounded in the presence of anti-Syt VII C_2A antibodies was severely affected.

The presence of EGTA or treatment with microtubule-depolymerizing drugs also inhibited plasma membrane resealing, as indicated by an increased uptake of the second dextran tracer after wounding. Under untreated conditions, 70%–75% of the wounded cells excluded the second tracer, after 1 min at 37°C. In contrast, only 35% of cells wounded in the presence of EGTA and 48% of cells wounded after nocodazole treatment excluded the second tracer. Again, these values were probably underestimated, since specific loss of wounded cells also occurred in these experiments (results not shown). The requirement for intact microtubules is consistent with previous reports of inhibition of plasma membrane repair by antibodies against the microtubule-based motor kinesin (Steinhardt et al., 1994).

Exocytosis of Lysosomes Is Required for the Rapid Resealing of Microinjection Wounds

We found that cell viability was severely affected when NRK cells were microinjected with anti-Syt VII C_2A antibodies. In several experiments, most cells injected with these affinity-purified antibodies were lost by detachment from the coverslip within 1–2 hr. In contrast, recovery of 70%–80% of the cells was routinely observed after parallel injections of identical amounts of preimmune rabbit IgG, or unrelated antibodies (not shown). To further characterize this finding, we monitored the effect of anti-Syt VII C_2A antibodies on plasma membrane resealing, immediately after wounding by microinjection. An immediate result of plasma membrane injury in eu-

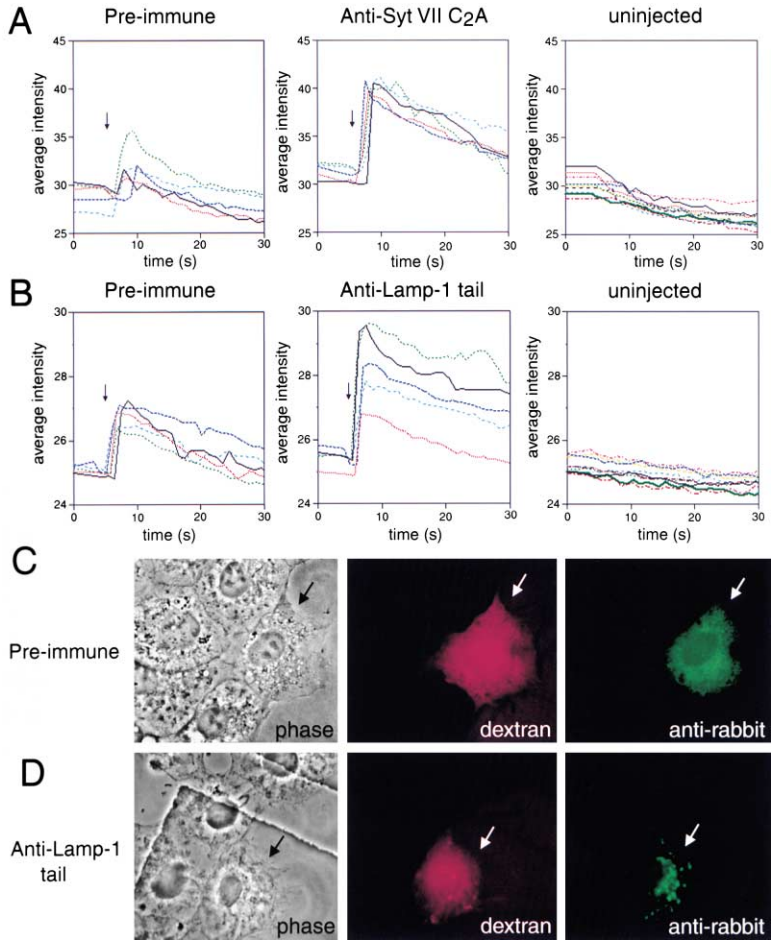

Figure 6. Exocytosis of Lysosomes Is Required for the Rapid Resealing of Microinjection Wounds

Fluo-3 AM-loaded NRK cells were subjected to time lapse fluorescence imaging, while microinjected with a Texas Red-dextran-solution containing preimmune or anti-Syt VII C_2A antibodies (A) or preimmune or anti-Lamp-1 cytosolic tail IgG (B). The average brightness intensity of a defined cytosolic region was measured on all time frames; arrows indicate when cells were injected. The brightness intensity of similar regions of uninjected cells was also analyzed, as a control for photobleaching. Data from 5 cells is shown for each condition; uninjected profiles correspond to 5 cells from preimmune injections, and 5 cells from anti-Syt VII C_2A or anti-Lamp-1 injections. After imaging, monolayers were fixed, permeabilized, and stained with anti-rabbit antibodies to reveal the preimmune (C) and anti-Lamp-1 tail (D) IgG injected into the cells. Phase contrast, Texas Red-dextran (red) and anti-rabbit IgG (green) images are shown; arrows point to microinjected cells.

karyotic cells is the influx of Ca^{2+}, down an approximately 10,000 fold concentration gradient. In this situation, Ca^{2+} levels rise and remain elevated until the plasma membrane is repaired, and cells can reestablish their normally low $[Ca^{2+}]_i$. To directly monitor this process, we loaded NRK cells with the fluorescent Ca^{2+} indicator Fluo 3-AM, and acquired sequential time-lapse fluorescence images (1 frame/s) while puncturing the plasma membrane with a microinjection needle. The average brightness intensity of Fluo 3-AM was measured on each image in a defined region of the cytoplasm, including the microinjection site. NRK cells microinjected with preimmune rabbit IgG showed a transient elevation in intracellular free Ca^{2+} immediately after membrane puncture, which lasted only a few seconds (Figure 6A, left), consistent with previous reports. When anti-Syt VII C_2A antibodies were injected, in contrast, a significantly brighter initial Ca^{2+} spike was detected, and the elevated Ca^{2+} levels were sustained throughout the 30 s period analyzed (Figure 6A, center). To determine the extent of photobleaching of the dye during this period, the brightness intensity of a defined region of the same size in uninjected cells present in the same microscopic field was also measured (Figure 6A, right). Taking into consideration that the 10%–15% reduction in brightness occurring between 10 and 30 s was due to photobleaching, the sustained high intracellular Ca^{2+} levels observed in cells microinjected with anti-Syt VII C_2A antibodies strongly suggest that plasma membrane resealing was severely impaired (Figures 6A–6C).

We subsequently utilized this antibody microinjection/Ca^{2+} imaging assay to test the involvement of lysosomal exocytosis in plasma membrane resealing, independently of Syt VII function. Previous studies showed that microinjection of antibodies against the eleven amino acid cytosolic tail of Lamp-1 results in extensive intracellular aggregation of lysosomes in NRK and other cell types. The distribution of other organelles, such as early and late endosomes and the Golgi complex, was not altered under the same conditions (Bakker et al., 1997; Rodríguez et al., 1996). We therefore reasoned that, if Ca^{2+}-triggered exocytosis of lysosomes is required for plasma membrane repair, microinjection of agglutinating anti-Lamp-1 tail antibodies should affect the rate of plasma membrane resealing. Confirming this prediction, rapid and sustained elevation in intracellular free Ca^{2+} was observed in four out of five cells injected with anti-Lamp-1 tail antibodies (Figure 6B, center), with the $[Ca^{2+}]_i$ reaching levels significantly higher than what was observed in cells microinjected with preimmune IgG (Figure 6B, left). Although similar to what was observed after microinjection of anti-Syt VII C_2A antibodies (Figure 6A, center), the results obtained with anti-Lamp-1 tail antibodies were more variable from cell to cell, consistent with a different inhibitory mechanism. After comple-

tion of time lapse imaging, the cells were fixed and stained with an anti-rabbit IgG fluorescent conjugate, allowing visualization of the diffuse cytoplasmic staining in cells microinjected with preimmune antibodies (Figure 6C), and of the aggregated lysosomes in cells microinjected with anti-Lamp-1 tail antibodies (Figure 6D).

Lysosomal Exocytosis Is Required for the Resealing of Skin Fibroblasts in a Collagen-Matrix Model of Wound Contraction

Having established that lysosomal exocytosis is required for the resealing of NRK cells wounded by contact with glass beads or microinjection, we proceeded to verify if the same mechanism was responsible for the repair of plasma membrane lesions induced in a physiological setting. The fibroblast-collagen-matrix contraction model (Grinnell, 2000; Tomasek et al., 1992) has been extensively used to study mechanisms that regulate wound contraction, a critical step in the healing of cutaneous lesions. In this model, analogous to the in vivo situation, primary skin fibroblasts embedded in a substrate-anchored collagen matrix form large extensions, abundant stress fibers, and develop isometric tension. During this process, collagen fibrils are reorganized and kept under mechanical pressure, as a result of force exerted by the cells. Release of the matrix from the substrate triggers rapid and synchronous contraction of the fibroblasts, with disappearance of stress fibers and retraction of pseudopodia (Mochitate et al., 1991; Tomasek et al., 1992). This contraction event causes compaction of the collagen matrix into a dense body one tenth of its original size, and induces generalized plasma membrane disruptions, presumably due to the rupture of focal adhesion sites. These lesions are rapidly resealed in a Ca^{2+}-dependent fashion, with the fibroblasts becoming again impermeable to extracellular tracers a few seconds after matrix contraction (Lin et al., 1997).

Substrate-anchored collagen matrices containing human foreskin fibroblasts were cultured for 48 hr, and either left anchored or released from the dish in the presence of Texas Red-dextran. Confocal laser scanning microscopy revealed that the fibroblasts in anchored matrices developed the expected extended morphology, with an intact plasma membrane (determined by exclusion of Texas Red-dextran), abundant actin stress fibers and negative surface staining for the lumenal domain of human Lamp-1. Upon matrix release from the substrate, the rapid contraction event was evident by a dramatic shortening of the cells, and disappearance of stress fibers. The majority of fibroblasts in released matrices suffered plasma membrane disruptions and incorporated Texas Red-dextran, as previously described (Lin et al., 1997). Similar to what was shown in Figure 1 for NRK, CHO, L6E9, and 3T3 cultured cell lines, the lumenal domain of Lamp-1 was detected with specific antibodies, on the surface of these wounded skin fibroblasts (Figure 7A).

The synchronous wounding of the majority of the fibroblast population during matrix contraction allowed us to simultaneously quantitate the release of the cytosolic enzyme lactate dehydrogenase (LDH), an indicator of plasma membrane disruptions, and β-hexosaminidase, a marker of lysosomal exocytosis (Rodríguez et al. 1997). β-hexosaminidase activity was detected in the supernatant shortly after the matrices were released from the substrate (0 min), but not when they remained attached (Figure 7B, top left panel). Consistent with previous results (Martinez et al., 2000), levels of β-hexosaminidase release from matrices lifted in the presence of anti-Syt VII C_2A domain antibodies were lower than those observed in the presence of preimmune rabbit IgG (Figure 7B, top center panel). A similar pattern was observed in the presence of recombinant C_2A domain fragments: the release of β-hexosaminidase detected shortly after the matrices were lifted was inhibited in the presence of Syt VII C_2A, and not in the presence of Syt I C_2A (Figure 7B, top right panel). LDH was only released in significant amounts while matrices were undergoing contraction (Figure 7B, lower left panel), as previously reported (Lin et al., 1997). Importantly, we found that LDH release from lifted matrices was much more robust in the presence of the inhibitory anti-Syt VII C_2A antibodies, when compared to preimmune rabbit IgG (Figure 7B, lower center panel). A similarly enhanced release of LDH was seen in the supernatants of matrices lifted in the presence of Syt VII C_2A, but not of Syt I C_2A (Figure 7B, lower right panel). In strong support of a role for lysosomes in plasma membrane repair, a precise correlation between lysosomal exocytosis (reflected by β-hexosaminidase release) and cell resealing (reflected by reduction in LDH release) was evident.

These experiments also revealed that the inhibition of plasma membrane resealing by anti-Syt VII C_2A antibodies or soluble Syt VII C_2A is reversible. After removal of the inhibitory reagents, the matrix fibroblasts were able to repair their plasma membranes and block LDH efflux (Figure 7B, lower panels). Furthermore, equal numbers of viable cells were subsequently recovered from these matrices (not shown). However, when Syt VII C_2A was kept in the medium after the matrices were released, the levels of LDH release from wounded fibroblasts remained elevated (Figure 7C, left panel). To examine the viability of fibroblasts wounded and incubated in the continuous presence of Syt VII C_2A, cells were harvested from contracted matrices by trypsin and collagenase treatment, recultured for 24 hr, and labeled with a pulse of [^{3}H]thymidine. Similar numbers of metabolically active cells were recovered from matrices incubated in the absence of any recombinant peptides, or in the presence of Syt I C_2A. In contrast, there was a significant reduction (of about 60%) in the number of viable fibroblasts recovered from contracted matrices incubated in the presence of the inhibitory Syt VII C_2A peptides (Figure 7C, right).

Discussion

Nature of the Exocytic Vesicles Responsible for Plasma Membrane Repair

Our results strongly suggest that Ca^{2+}-regulated exocytosis of conventional lysosomes mediates plasma membrane repair after injury. The following lines of evidence support this conclusion: (1) the strictly Ca^{2+}-dependent appearance of the lumenal domain of Lamp-1 on the cell surface, at the sites of plasma membrane disruption; (2) the exposure of the ectodomain of Syt VII, a synaptotagmin isoform previously localized on

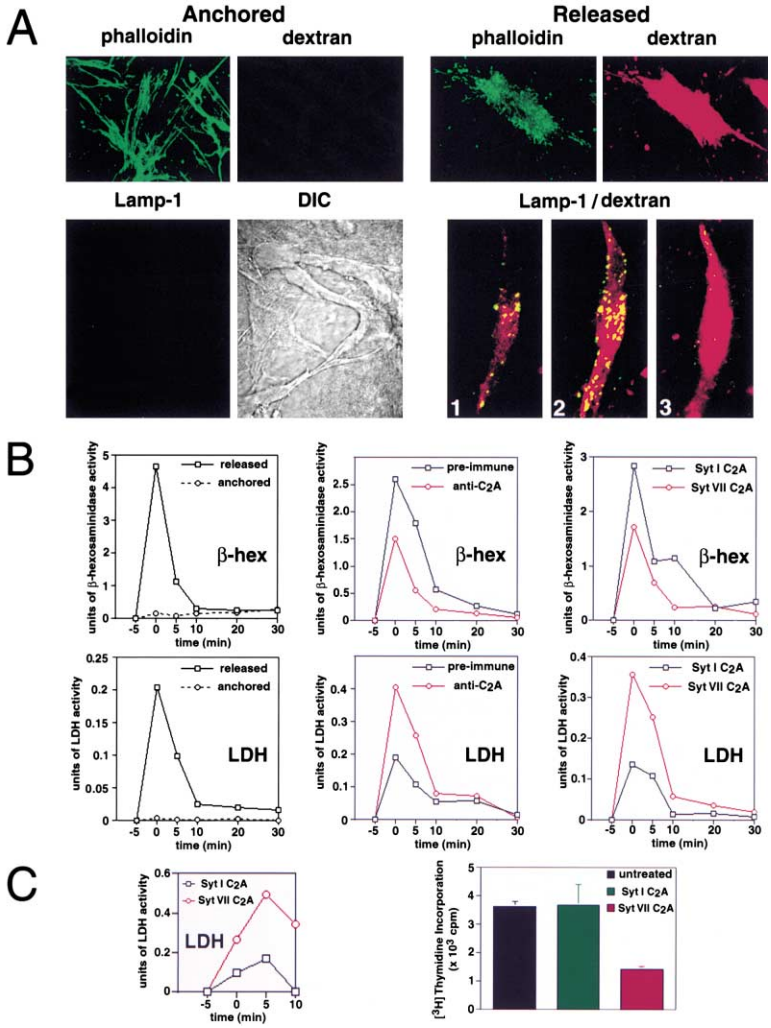

Figure 7. Lysosomal Exocytosis Mediates the Resealing of Skin Fibroblasts Wounded during Collagen Matrix Contraction

(A) Fibroblast-collagen matrices remaining anchored or released in the presence of Texas Red-dextran were permeabilized and stained with fluorescein-phalloidin (top), or surface-labeled with anti-Lamp-1 mAbs (bottom), and analyzed by confocal microscopy. Release-triggered contraction is evident by the phalloidin-stained F actin transition from fibrilar (anchored matrices), to granulated (released matrices). Cytosolic incorporation of Texas Red-dextran (top right) and surface Lamp-1 labeling were detected on optical sections through the surface (bottom right, 1 and 2) but not the cell center (bottom right, 3). Fibroblasts in anchored matrices had no cytosolic Texas Red-dextran (top left) and no surface Lamp-1 (bottom left). DIC image shows dextran-free cells embedded in an anchored collagen matrix.

(B) β-hexosaminidase and LDH activity were measured in the supernatant of anchored (left, interrupted black lines) or released matrices (left, solid black), and in the supernatant of matrices released in the presence of Syt VII C_2A or anti-Syt VII C_2A antibodies (center and right, red), or of Syt I C_2A or preimmune rabbit antibodies (center and right, black). Data corresponds to the average of duplicates.

(C) C_2A domain peptides were kept in the medium during and after fibroblast contraction, and the released LDH activity (left) and [^{3}H]thymidine incorporation after fibroblast harvest and reculture (right) were determined. The continuous presence of Syt VII C_2A resulted in sustained release of LDH (left, red) and reduced fibroblast viability (right, red). Data corresponds to the average of duplicate (left) or triplicates +/− SD (right).

lysosomes, on the cell surface after wounding; (3) the inhibition of Lamp-1 surface exposure and plasma membrane repair by antibodies against the Syt VII C_2A domain, or soluble Syt VII C_2A; (4) the defect in plasma membrane resealing observed after microinjection of agglutinating antibodies specific for the cytosolic domain of Lamp-1; and (5) the finding that Syt VII-dependent exocytosis of lysosomes is required for the resealing of primary skin fibroblasts wounded during contraction of collagen matrices.

Previous studies showed that Ca^{2+} influx through plasma membrane lesions triggers a highly localized exocytic response in a variety of animal cells (Bi et al., 1995; Miyake and McNeil, 1995; Steinhardt et al., 1994; Togo et al., 1999). However, the exact nature of the intracellular vesicles involved in this process remained, until now, obscure. In light of our present findings, those earlier observations are fully consistent with the general conclusion that lysosomes correspond to the vesicular population responsible for plasma membrane resealing. The intracellular vesicles mobilized for exocytosis during the wounding of endothelial cells and fibroblasts were actually suggested to belong to the endosomal/lysosomal compartment, based on labeling with the endocytic tracer FM-143. However, the very long continuous dye uptake periods utilized in those studies did not allow a more precise identification of the vesicular compartment involved (Miyake and McNeil, 1995; Togo et al., 1999). In sea urchin eggs, although plasma membrane repair was initially proposed to be mediated by exocytosis of cortical granules (Bi et al., 1995), the resealing of larger lesions was shown to require yolk granule exocytosis (McNeil et al., 2000). Interestingly, yolk granules from eggs of several species are acidic compartments, accessible through the endocytic pathway and containing lysosomal hydrolases (Busson-Mabillot, 1984; Hart et al., 1987; Wall and Meleka, 1985). Finally, based on the inhibition in resealing observed after brefeldin A treatment, vesicles derived from the Golgi apparatus were also recently proposed to play a role (Togo et al., 1999). It is important to note, however, that in addition to its effects on the Golgi apparatus, brefeldin A also alters the morphology and functional properties of lysosomes (Lippincott-Schwartz et al., 1991).

Lysosomes as Ca^{2+}-Dependent Exocytic Vesicles Regulated by Synaptotagmin VII

Recent investigations of the molecular machinery involved in Ca^{2+}-regulated exocytosis of lysosomes implicated Syt VII, a ubiquitously expressed member of the synaptotagmin family of putative Ca^{2+} sensors (Caler et al., 2001; Martinez et al., 2000). Recently proposed

models for the role of the neuronal synaptotagmin isoform Syt I in the regulation of synaptic vesicle exocytosis suggest that Ca^{2+}-triggered interactions involving the C_2 domains alter the physical relationship between the SNARE complex and lipid bilayers, facilitating fusion (Davis et al., 1999; Gerona et al., 2000). Although it remains to be determined if Syt VII acts in a similar fashion in lysosomal exocytosis, the ability to modulate Syt VII function provided us with a tool to directly verify if Ca^{2+}-regulated exocytosis of lysosomes was responsible for plasma membrane resealing.

We initially used specific anti-Syt VII ectodomain antibodies (Martinez et al., 2000) in surface-staining assays to show that this synaptotagmin isoform is, similar to Lamp-1, exposed on the cell surface after cell wounding. Results from a series of subsequent experiments strongly suggested that Syt VII, thorough its C_2A domain, plays an important functional role in the exocytosis of lysosomes triggered by wounding, and in plasma membrane repair. When cells were injured in the presence of recombinant C_2A domain of Syt VII, or affinity-purified antibodies against this domain, Lamp-1 surface exposure was specifically inhibited, and the cells showed a clear defect in plasma membrane resealing. These results are consistent with a recent report describing inhibition of plasmalemma repair in severed neurites of PC-12 cells by anti-synaptotagmin C_2A antibodies (Detrait et al., 2000). Although those antibodies were generated against the C_2A domain of squid synaptotagmin (Detrait et al., 2000), the high degree of sequence conservation among synaptotagmin C_2A domains is consistent with the possibility that the ubiquitously expressed Syt VII was targeted in those studies.

The dramatic inhibitory effect of anti-Syt VII C_2A antibodies on plasma membrane resealing was directly visualized in imaging experiments, which revealed a significantly more intense and sustained Ca^{2+} influx following microinjection, when compared to cells microinjected with preimmune IgG. This assay also allowed us to confirm, independently of Syt VII function, that lysosomes are directly involved in plasma membrane resealing. A sharper and sustained elevation in $[Ca^{2+}]_i$ was observed after microinjection of antibodies against the cytosolic tail domain of Lamp-1, previously shown to specifically agglutinate lysosomes when introduced into live cells (Bakker et al., 1997; Rodríguez et al., 1996).

Wounding and Resealing of Skin Fibroblasts during Contraction of Collagen Matrices

The fundamental process of cutaneous wound healing involves three steps: epithelization (to resurface the wound), connective tissue deposition (to replace damaged dermis), and contraction (to bring the margins of the wound together). Skin fibroblasts, the cells responsible for wound contraction, are normally sessile and quiescent. However, when a cutaneous wound occurs, skin fibroblasts become activated, migrate to the fibronectin-fibrin wound interface, proliferate, and synthesize granulation tissue, a new collagen-containing matrix. Within the granulation tissue, the fibroblasts develop strong focal adhesions, actin stress fibers, and generate force, which ultimately leads to contraction of the wound. After contraction is completed, the tension is released, concurrently with the transition from granulation tissue into dermis, or scar tissue (Grinnell, 1994). This process of collagen matrix contraction followed by transition into a mechanically relaxed tissue has been extensively studied using an in vitro culture model (Grinnell, 1994, 2000; Tomasek et al., 1992). In this system, the release in tension that follows lifting of fibroblast-collagen matrices from the substrate results in a synchronous contraction event, which causes transient plasma membrane disruptions in the majority of the fibroblasts (Lin et al., 1997). Here, we showed that vigorous, Syt VII-dependent exocytosis of lysosomes occurs upon contraction-induced wounding of fibroblasts in collagen matrices, and that this event is required for the rapid repair of their plasma membrane lesions.

A Microbiological Link?

It has been proposed that exocytosis triggered by Ca^{2+} influx through plasma membrane wounds may have preceded more specialized forms of secretion (McNeil and Steinhardt, 1997; McNeil and Terasaki, 2001). This basic strategy for resealing may have evolved as a result of a variety of selection pressures, including the self-evident need of cells to survive in mechanically challenging environments. In this scenario, an intriguing idea is that lysosomes may have provided an additional advantage in the repair of cellular membranes damaged by microbes. Secretion of "harmful" lysosomal contents could have represented an early defense mechanism against bacteria producing pore-forming toxins, and other membrane-disrupting agents. Recent reports actually highlight the fact that large parasites such as *Plasmodium yoelii* and *Trichinella spiralis* also induce plasma membrane wounds, as they move through host tissues (Mota et al., 2001; Butcher et al., 2000).

Experimental Procedures

Cell Culture

NRK, 3T3, and L6E9 cells were grown in DMEM, and CHO cells in α-MEM, with 10% fetal bovine serum (FBS), at 37°C in 5% CO_2. Cells were plated on glass coverslips at 48 hr, and grown to 6×10^4 cells/cm^2 prior to scratch, scrape, and glass bead wounding experiments. Fibroblasts from human foreskin specimens (<10 passages) were obtained from the Cell Culture Core facility, Yale Skin Diseases Research Center, and maintained in DMEM 10% FBS.

Antibodies and Recombinant Proteins

Rabbit polyclonal antibodies against the NH_2-terminal or C_2A domains of Syt VII, or the COOH-terminal domain of Lamp-1 were generated and affinity purified as previously described (Martinez et al., 2000; Rodríguez et al., 1996). Anti-rat Lamp-1 lumenal epitope hybridoma LYIC6 was kindly provided by Ira Mellman (Department of Cell Biology, Yale University). Anti-mouse (1D4B), human (H4A3), and hamster (UH1) Lamp-1 lumenal epitope mAbs were obtained from the Developmental Studies Hybridoma Bank. The C_2A domains of Syt VII and Syt I were cloned into pET19b (Novagen) as previously described (Martinez et al., 2000). Polyhistidine-tagged fusion proteins were expressed in *E. coli* BL21 and purified on nickel-agarose, according to manufacturer's instructions (Novagen).

Scratch Wound and Staining for Surface Lamp-1 and Syt VII

Monolayers were rinsed, placed on a heated stage at 37°C, and covered with 30 μl of 5 mg/ml lysine-fixable 10 kDa Texas Red-dextran (Molecular Probes) in PBS, or in PBS containing 10 μM nocodazole, 200 μg/ml recombinant Syt VII C_2A or Syt I C_2A, 20 μg/ml anti-Syt VII C_2A or preimmune rabbit IgG, or Ca^{2+}-free PBS

containing 10 mM EGTA. Cells were wounded by scratching 20 times in a grid pattern with a single-edge surgical blade (Becton Dickinson), transferred to ice, and incubated for 30 min with LYIC6, 1D4B, or UH1 hybridoma supernatant, or 20 μg/ml anti-Syt VII C_2A, or anti-Syt VII NH_2-terminus IgG. After rinsing in cold PBS, cells were fixed with 2% paraformaldehyde (PFA) and incubated with Alexa 488-goat anti-mouse antibodies (Molecular Probes) for 30 min, and with DAPI (Sigma) for 3 min. For labeling of permeabilized cells with anti-Syt VII C_2A, fixed cells were permeabilized with 0.1% Triton X-100 for 10 min (Martinez et al., 2000) prior to incubation with antibodies. Images were acquired on a Zeiss axiovert 135 microscope equipped with an Orca II digital camera (Hamamatsu) controlled by Metamorph software (Universal Imaging). For each of triplicate coverslips, all cells in 14 fields at 100× magnification were enumerated according to positive DAPI, Texas Red-dextran and anti-Lamp-1 surface staining. Optical Z sections of 0.45 μm were acquired on a laser scanning confocal microscope (Zeiss Axiovert LSM 510).

Microinjection, Staining for Surface Lamp-1, and Time Lapse Fluorescence Imaging

NRK cells were plated at a density of 1×10^4 cells/cm^2 on gridded coverslips (CELLocate, Eppendorf), cultured for 48 hr, transferred to DMEM 1% BSA 20 mM HEPES (pH 7.0) and placed at 37°C on a heated microscope stage. Texas Red-dextran (1 mg/ml in 27 mM K_2HPO_4, 8 mM Na_2HPO_4, and 26 mM KH_2PO_4, [pH 7.2]) was microinjected into approximately 40–60 cells within 3 min using a 5242 microinjector, 5170 micromanipulator (Eppendorf) and finely pulled glass capillaries with a tip opening diameter of 0.5 ± 0.2 μm (Femtotips, Eppendorf). Microinjected cells were immediately incubated with LY1C6 hybridoma supernatant at 4°C for 30 min, fixed with 2% PFA and incubated with Alexa 488-goat anti-mouse antibodies (Molecular Probes) for 30 min. Images were acquired using a Zeiss LSM 510 laser scanning confocal microscope, as detailed above.

For time lapse imaging of $[Ca^{2+}]_i$, NRK cells were loaded with 5 μM Fluo-3-AM, 0.5% pluronic F-127, and 0.5 mM probenecid for 45 min in DMEM 10% FBS. After washing, coverslips were transferred to DMEM 1% BSA 20 mM HEPES (pH 7.0), and kept at 37°C on a heated microscope stage. The microinjection needle was positioned on a specific cell site, and a phase image was acquired to determine the injection site. Cells were then injected with 1 mg/ml Texas Red-dextran in microinjection buffer, or in microinjection buffer containing 1 mg/ml anti-Syt VII C_2A, anti-Lamp-1 cytosolic tail or purified preimmune rabbit IgG. Fluorescent images (100 ms exposure, Orca II digital camera, Hamamatsu) were collected through a 30× objective, at time-lapse intervals of 1 s using a computer-controlled shutter system. The average brightness intensity in a defined area around the microinjection site of each cell was determined on all frames of the stack, using Metamorph software (Universal Imaging). At the end of time lapse imaging, cells were fixed in 2% PFA, permeabilized with 0.05% saponin, and stained with Alexa 488-goat anti-rabbit antibodies (Molecular Probes) for 30 min.

Scrape Wounding, Staining for Surface Lamp-1, and Flow Cytometry

Cells were rinsed, placed on a heated stage at 37°C, and covered with 100 μl of 5 mg/ml lysine fixable, 10 kDa BODIPY FL-dextran (Molecular Probes) in PBS, or PBS containing 200 μg/ml recombinant Syt VII C_2A or Syt I C_2A, 20 μg/ml anti-Syt VII C_2A or preimmune rabbit IgG, or Ca^{2+}-free PBS containing 10 mM EGTA. Cells were resuspended by scraping 10 times with a 1.8 cm blade cell scraper (Becton Dickinson), 5 ml cold PBS was added, cells were centrifuged, resuspended in 50 μl cold LY1C6 hybridoma supernatant, and incubated at 4°C for 30 min. Cells were then washed, fixed with 2% PFA, stained with R-Phycoerythrin-goat anti-mouse antibodies (Molecular Probes) for 30 min, resuspended in 0.3 ml PBS and analyzed by flow cytometry. A fluorescence-activated cell sorter (FACS) Vantage Flow Cytometer (Becton-Dickinson Immunocytometry Systems) was used to excite the cells at 488 nm, and the BODIPY-FL and Phycoerythrin fluorescent emission was collected through 530/30 and 575/26 nm band pass filters, respectively. A minimum of 10,000 cells was analyzed in each sample. Data analysis was performed using CellQuest (Becton-Dickinson).

Glass Bead Wounding and Resealing Assay

Coverslips were placed on a 37°C stage, covered with 50 μl of 5 mg/ml 10 kDa Texas Red-dextran in PBS (containing or not 200 μg/ml recombinant Syt VII C_2A or Syt I C_2A, or 20 μg/ml anti-Syt VII C_2A or preimmune rabbit IgG), and sprinkled with 0.05 g (~200 beads) of acid-washed glass beads (425–600 μm, Sigma). The coverslips were gently rocked 4 times to let the beads roll over the cells, rinsed in PBS and either incubated immediately with 50 μl of 5 mg/ml BODIPY FL-dextran in PBS for 15 s, or after incubation in PBS for 1 or 3 min at 37°C. Recombinant C_2A peptides or antibodies were kept in the medium during all incubation steps. Cells were then rinsed with cold PBS, fixed with 2% PFA, and DAPI stained. Resealing experiments in cells pretreated with nocodazole (10 μM, 30 min at 4°C) or in the presence of EGTA (10 mM) were performed as described above, except that cells were wounded by scratching. The number of Texas Red-positive and BODIPY FL-positive cells in the total cell population was counted in 14 fields at 100× magnification, in triplicate.

Fibroblast-Mediated Contraction of Collagen Matrices

Neutralized Vitrogen 100 collagen (Cohesion Corp.) solutions were prepared at 1.5 mg/ml in serum-free DMEM containing 5×10^6 human foreskin fibroblasts/ml, as previously described (Lin et al. 1997). Aliquots (0.2 ml) of the cell/collagen mixtures were warmed at 37°C for 5 min and placed in a 12 mm diameter area within each well of a 24-well plate. After 60 min incubation at 37°C /5% CO_2 to allow collagen polymerization, 1 ml DMEM 10% FBS containing 50 μg/ml ascorbic acid (Sigma) was added, and matrices were further incubated for 48 hr. To trigger fibroblast contraction and wounding, anchored collagen matrices were released from the culture dishes by inserting a thin spatula between the matrix and the dish surface, in the presence of Texas Red-dextran (Lin et al. 1997). Released and anchored matrices were rinsed extensively, fixed with 2% PFA, permeabilized with 0.5% Triton X-100 for 10 min, and incubated for 30 min with 1 U of fluorescein-phalloidin (Molecular Probes). Immediately after release and contraction (or not, for anchored matrices), extensive cold PBS rinses were performed followed by 30 min incubation at 4°C with H4A3 hybridoma supernatant. Matrices were then rinsed in cold PBS, fixed with 2% PFA and incubated with Alexa 488-goat anti-mouse antibodies for 30 min. After washing, matrices were mounted on glass slides with gel-mount (Biomeda corp.) and confocal optical Z sections of 0.30 μm were acquired.

Lactate Dehydrogenase and β-Hexosaminidase Activity Assays

Collagen-fibroblast matrices were preincubated for 30 min at 37°C in Ringer's 1% BSA (Rodríguez et al., 1999) containing 200 μg/ml recombinant Syt VII C_2A or Syt I C_2A, or 20 μg/ml anti-Syt VII C_2A or preimmune IgG. The incubation media was collected before (−5 min time point) and after contraction, followed by replacement with an equal volume (0.5 ml) of fresh Ringer's-BSA. LDH activity in duplicate 50 μl supernatant samples was determined using CytoTox 96® (Promega). Background levels of LDH activity detected prewounding (not higher than 15% of peak values) were subtracted from each value. β-hexosaminidase activity was determined by incubating duplicate 100 μl supernatant samples with 0.4 ml of 2 mM 4-methyl-umbellyferyl-*N*-acetyl-β-D-glucosaminide (Sigma), as previously described (Martinez et al., 2000). Background levels of β-hexosaminidase activity detected prewounding (not higher than 10% of peak values) were subtracted from each sample.

DNA Synthesis

Collagen-fibroblast matrices were preincubated for 30 min at 37°C in Ringer's-BSA, or Ringer's-BSA containing 200 μg/ml recombinant Syt VII C_2A or Syt I C_2A released from the dish to initiate contraction and wounding, and incubated in the same media for an additional 2 hr at 37°C. Fibroblasts were then harvested from matrices with trypsin and collagenase treatment as previously described (Lin et al., 1997), cultured overnight at 37°C and radiolabeled metabolically for 2 hr at 37°C with 5 μCi/ ml methyl-[^{3}H]thymidine (20 Ci/mmol,

Amersham Life Science). The cultures were rinsed, DNA was precipitated with 10% trichloroacetic acid for 5 min at 4°C, and dissolved in 0.5 ml 0.25 M NaOH/1% SDS. The radioactivity of 0.1 ml samples mixed with 5 ml SafeScint (American Bioanalytical) was determined in a liquid scintillation counter (Wallac 1409).

Acknowledgments

We are very grateful to P. McNeil for advice with cell wounding, and to F. Grinnell and C-H. Ho for help with fibroblast-collagen-matrix contraction experiments. We also thank S. Chakrabarti for Syt VII and Syt I C_2A recombinant constructs; R. Tigelaar for human foreskin fibroblasts; B. Burleigh, J. Kagan, A. Rodríguez, and members of the Andrews, Galán, and Roy laboratories for helpful suggestions; R. Carbone for flow cytometry; P. De Camilli for Syt I plasmids; I. Mellman for the LYIC6 hybridoma; and H. Tan for excellent technical assistance. This work was supported by a grant from the NIH (AI34867) and a Burroughs Welcome Scholar Award to N.W.A.

Received January 10, 2001; revised June 21, 2001.

References

Andrews, N.W. (2000). Regulated secretion of conventional lysosomes. Trends Cell Biol. *10*, 316–321.

Bakker, A.C., Webster, P., Jacob, W.A., and Andrews, N.W. (1997). Homotypic fusion between aggregated lysosomes triggered by elevated $[Ca^{2+}]_i$ in fibroblasts. J. Cell Sci. *110*, 2227–2238.

Bi, G.Q., Alderton, J.M., and Steinhardt, R.A. (1995). Calcium-regulated exocytosis is required for cell membrane resealing. J. Cell Biol. *131*, 1747–1758.

Bodemann, H., and Passow, H. (1972). Factors controlling the resealing of the membrane of human erythrocyte ghosts after hypotonic hemolysis. J. Membr. Biol. *8*, 1–26.

Busson-Mabillot, S. (1984). Endosomes transfer yolk proteins to lysosomes in the vitellogenic oocyte of the trout. Biol. Cell *51*, 53–66.

Butcher, B.A., Gagliardo, L.F., Warren, T., and Appleton, J.A. (2000). Larvae-induced plasma membrane wounds and glycoprotein deposition are insufficient for Trichinella spiralis invasion of epithelial cells. Mol. Biochem. Parasitol. *107*, 207–218.

Caler, E.V., Chakrabarti, S., Fowler, K.T., Rao, S., and And Andrews, N.W. (2001). The exocytosis-regulatory protein synaptotagmin VII mediates cell invasion by *Trypanosoma cruzi*. J. Exp. Med. *193*, 1097–1104.

Chang, D.C., and Reese, T.S. (1990). Changes in membrane structure induced by electroporation as revealed by rapid-freezing electron microscopy. Biophys. J. *58*, 1–12.

Chavez, R.A., Miller, S.G., and Moore, H.P. (1996). A biosynthetic regulated secretory pathway in constitutive secretory cells. J. Cell Biol. *133*, 1177–1191.

Chen, W.T. (1981). Surface changes during retraction-induced spreading of fibroblasts. J. Cell Sci. *49*, 1–13.

Coorsen, J.R., Schmitt, H., and Almers, W. (1996). Ca^{2+} triggers massive exocytosis in Chinese hamster ovary cells. EMBO J. *15*, 3787–3791.

Dai, J., and Sheetz, M.P. (1995). Regulation of endocytosis, exocytosis, and shape by membrane tension. Cold Spring Harb. Symp. Quant. Biol. *60*, 567–571.

Davis, A.F., Bai, J., Fasshauer, D., Wolowick, M.J., Lewis, J.L., and Chapman, E.R. (1999). Kinetics of synaptotagmin responses to Ca^{2+} and assembly with the core SNARE complex onto membranes. Neuron *24*, 363–376.

Detrait, E.R., Yoo, S., Eddleman, C.S., Fukuda, M., Bittner, G.D., and Fishman, H.M. (2000). Plasmalemmal repair of severed neurites of PC12 cells requires Ca^{2+} and synaptotagmin. J. Neurosc. Res. *62*, 566–573.

Eddleman, C.S., Ballinger, M.L., Smyers, M.E., Godell, C.M., Fishman, H.M., and Bittner, G.D. (1997). Repair of plasmalemmal lesions by vesicles. Proc. Natl. Acad. Sci. USA *94*, 4745–4750.

Gerona, R.R., Larsen, E.C., Kowalchyk, J.A., and Martin, T.F. (2000). The C terminus of SNAP25 is essential for Ca^{2+}-dependent binding of synaptotagmin to SNARE complexes. J. Biol. Chem. *275*, 6328–6336.

Grinnell, F. (1994). Fibroblasts, myofibroblasts, and wound contraction. J. Cell Biol. *124*, 401–404.

Grinnell, F. (2000). Fibroblast-collagen matrix contraction: growth factor signalling and mechanical loading. Trends Cell Biol. *10*, 362–365.

Hart, N.H., Wolenski, J.S., and Donovan, M.J. (1987). Ultrastructural localization of lysosomal enzymes in the egg cortex of Brachydanio. J. Exp. Zool. *244*, 17–32.

Harter, C., and Mellman, I. (1992). Transport of the lysosomal glycoprotein lgp120 (lgpA) to lysosomes does not require appearance on the plasma membrane. J. Cell Biol. *117*, 311–325.

Kasai, H., Kishimoto, T., Liu, T.-T., Miyashita, Y., Podini, P., Grohovaz, F., and Meldolesi, J. (1999). Multiple and diverse forms of regulated exocytosis in wild type and defective PC12 cells. Proc. Natl. Acad. Sci. USA *96*, 945–949.

Lee, B., McKenna, K., and Bramhall, J. (1985). Kinetic studies of human erythrocyte membrane resealing. Biochim. Biophys. Acta *815*, 128–134.

Li, C., Ullrich, B., Zhang, J.Z., Anderson, R.G.W., Brose, N., and Sudhof, T.C. (1995). Ca^{2+}-dependent and independent activities of neural and non-neural synaptotagmins. Nature *375*, 594–599.

Lieber, M.R., and Steck, T.L. (1982). Dynamics of the holes in human erythrocyte membrane ghosts. J. Biol. Chem. *257*, 11660–11666.

Lin, Y.C., Ho, C.H., and Grinnell, F. (1997). Fibroblasts contracting collagen matrices form transient plasma membrane passages through which the cells take up fluorescein isothiocyanate-dextran and Ca^{2+}. Mol. Biol. Cell *8*, 59–71.

Lippincott-Schwartz, J., Yuan, L., Tipper, C., Amherdt, M., Orci, L., and Klausner, R.D. (1991). Brefeldin A's effects on endosomes, lysosomes, and the TGN suggest a general mechanism for regulating organelle structure and membrane traffic. Cell *67*, 601–616.

Martinez, I., Chakrabarti, S., Hellevik, T., Morehead, J., Fowler, K., and Andrews, N.W. (2000). Synaptotagmin VII regulates Ca(2+)-dependent exocytosis of lysosomes in fibroblasts. J. Cell Biol. *148*, 1141–1149.

McNeil, P.L., and Ito, S. (1989). Gastrointestinal cell plasma membrane wounding and resealing in vivo. Gastroenterology *96*, 1238–1248.

McNeil, P.L., and Khakee, R. (1992). Disruptions of muscle fiber plasma membranes. Role in exercise-induced damage. Am. J. Pathol. *140*, 1097–1109.

McNeil, P.L., and Steinhardt, R.A. (1997). Loss, restoration and maintenance of plasma membrane integrity. J. Cell Biol. *137*, 1–4.

McNeil, P.L., and Terasaki, M. (2001). Coping with the inevitable: how cells repair a torn surface membrane. Nature Cell Biol. *3*, E124–129.

McNeil, P.L., and Warder, E. (1987). Glass beads load macromolecules into living cells. J. Cell Sci. *88*, 669–678.

McNeil, P.L., Murphy, R.F., Lanni, F., and Taylor, D.L. (1984). A method for incorporating macromolecules into adherent cells. J. Cell Biol. *98*, 1556–1564.

McNeil, P.L., Vogel, S.S., Miyake, K., and Terasaki, M. (2000). Patching plasma membrane disruptions with cytoplasmic membrane. J. Cell Sci. *113*, 1891–1902.

Mikoshiba, K., Fukuda, M., Moreira, J.E., Lewis, F.M., Sugimori, M., Niinobe, M., and Llinas, R. (1995). Role of the C2A domain of synaptotagmin in transmitter release as determined by specific antibody injection into the squid giant synapse preterminal. Proc. Natl. Acad. Sci. USA *92*, 10703–10707.

Miyake, K., and McNeil, P.L. (1995). Vesicle accumulation and exocytosis at sites of plasma membrane disruption. J. Cell Biol. *131*, 1737–1745.

Mochitate, K., Pawelek, P., and Grinnell, F. (1991). Stress relaxation of contracted collagen gels: disruption of actin filament bundles, release of cell surface fibronectin, and down-regulation of DNA and protein synthesis. Exp. Cell Res. *193*, 198–207.

Mota, M.M., Pradel, G., Vanderberg, J.P., Hafalla, J.C., Frevert, U., Nusenzweig, R.S., Nussenzweig, V., and Rodríguez, A. (2001). Migration of Plasmodium sporozoites through cells before infection. Science *291*, 141–144.

Ninomiya, Y., Kishimoto, T., Miyashita, Y., and Kasai, H. (1996). Ca^{2+}-dependent exocytic pathways in Chinese Hamster Ovary fibroblasts revealed by a caged-Ca^{2+} compound. J. Biol. Chem. *271*, 17751–17754.

Rodríguez, A., Samoff, E., Rioult, M.G., Chung, A., and Andrews, N.W. (1996). Host cell invasion by trypanosomes requires lysosomes and microtubule/kinesin-mediated transport. J. Cell Biol. *134*, 349–362.

Rodríguez, A., Webster, P., Ortego, J., and Andrews, N.W. (1997). Lysosomes behave as Ca^{2+}-regulated exocytic vesicles in fibroblasts and epithelial cells. J. Cell Biol. *137*, 93–104.

Rodríguez, A., Martinez, I., Chung, A., Berlot, C.H., and Andrews, N.W. (1999). cAMP regulates Ca^{2+}-dependent exocytosis of lysosomes and lysosome-mediated cell invasion by trypanosomes. J. Biol. Chem. *274*, 16754–16759.

Schiavo, G., Osborne, S.L., and Sgouros, J.G. (1998). Synaptotagmins: more isoforms than functions? Biochem. Biophys. Res. Commun. *248*, 1–8.

Steinhardt, R.A., Guoqiang, B., and Alderton, J.M. (1994). Cell membrane resealing by a vesicular mechanism similar to neurotransmitter release. Science *263*, 390–393.

Sudhof, T.C., and Rizo, J. (1996). Synaptotagmins: C2-domain proteins that regulate membrane traffic. Neuron *17*, 379–388.

Sugita, S., and Sudhof, T.C. (2000). Specificity of Ca^{2+}-dependent protein interactions mediated by the C2A domains of synaptotagmins. Biochemistry *39*, 2940–2949.

Swanson, J.A., and McNeil, P.L. (1987). Nuclear reassembly excludes large macromolecules. Science *238*, 548–550.

Terasaki, M., Miyake, K., and McNeil, P.L. (1997). Large plasma membrane disruptions are rapidly resealed by Ca^{2+}-dependent vesicle-vesicle fusion events. J. Cell Biol. *139*, 63–74.

Togo, T., Alderton, J.M., Bi, G.Q., and Steinhardt, R.A. (1999). The mechanism of facilitated cell membrane resealing. J. Cell Sci. *112*, 719–731.

Togo, T., Krasieva, T.B., and Steinhardt, R.A. (2000). A decrease in membrane tension precedes successful cell-membrane repair. Mol. Biol. Cell *11*, 4339–4346.

Tomasek, J.J., Haaksma, C.J., Eddy, R.J., and Vaughan, M.B. (1992). Fibroblast contraction occurs on release of tension in attached collagen lattices: dependency on an organized actin cytoskeleton and serum. Anat. Rec. *232*, 359–368.

Ullrich, B., and Sudhof, T.C. (1995). Differential distributions of novel synaptotagmins: comparison to synapsins. Neuropharmacology *34*, 1371–1377.

Wall, D.A., and Meleka, I. (1985). An unusual lysosome compartment involved in vitellogenin endocytosis by Xenopus oocytes. J. Cell Biol. *101*, 1651–1664.